

CHAPTER 3

Characterization and Beneficiation (Experimental-I)

Types and sources of Iron and Steel Plant's wastes are discussed in Chapter one and two. This chapter deals with the characterization of raw materials (which include sieve analysis of Steel Plant's wastes (i.e.dust and sludge), chemical analysis of dust and sludge, and proximate analysis of coal etc.By beneficiation methods, an attempt was made to find suitable up-gradation technique to increase the total Fe percentage of dust and sludge; thereby to develop a proper beneficiation method for dust and sludge.

3.1 Characterization and Preparations of Raw Materials

In any experimental work, it is extremely important to characterize the input materials as they provide necessary information required for assessment of the properties of the products. These include evaluation of physical, chemical, and other characteristics of the materials. The sources of raw materials used for experimental work are shown in Table 3.1.

Table 3.1: Sources of Raw Materials

Sources of Iron Oxide (Steel Plant's wastes)	
Steel melting shop dust	Jindal Steel Works, Bellari, Karnataka, India
Steel melting shop sludge	Jindal Steel Works, Bellari, Karnataka, India
Steel melting shop sludge	Vizag Steel Plant, Vishakhapatnam, Andhra Pradesh, India
Coal	

Coal	Procured from local market
Binder	
Lime	Procured from local market (laboratory reagent grade)
Fly ash	Thermal Power Plant, Vanakbori, Gujarat.
Molasses	Procured from local Foundry
Starch	Procured from local market

3.2 Instrument/Apparatus Used for Characterization and Beneficiation

There are different instrument or apparatus used for characterization and beneficiation of raw materials:

1. Sieve shaker,
2. Ball mill,
3. X-ray Fluorescence (XRF) Spectrometer,
4. Scanning electron microscopy (SEM),
5. X-ray diffractometer,
6. Air classifier,
7. Centrifugal classifier,
8. Wilfley Tabling.

3.2.1 Sieve Shaker

Sieve analysis is one the oldest methods of size analysis and is accompanied by passing a known weight of sample material successively through number of sieves. After specified time for sieving, weights are taken of the collecting material on each sieve to determine the percentage of each size fraction. The effectiveness of a size analysis depends on the amount of material, i.e. charge, put on the sieve and the type of movement imparted to the sieve shaker. Sieves are designated by the nominal aperture size, which is the nominal central separation of opposite sides of acquire aperture or the nominal diameter of a round aperture. A variety of sieve aperture ranges are currently used, the most popular standards are BSS 410, ASTM standard, DIN 4188, German Standard etc. Table 3.2 shows the BSS 410 standard for wire-mesh sieves.

Table3.2: BSS 410 Standard

Mesh number	Nominal aperture size (μm)	Mesh number	Nominal aperture size (μm)
3	5600	36	425
3.5	4750	44	355
4	4000	52	300
5	3350	60	250
6	2800	72	212
7	2360	85	180
8	2000	100	150
10	1700	120	125
12	1400	150	106
14	1180	170	90
16	1000	200	75
18	850	240	63
22	710	300	53
25	600	350	45
30	500	400	38



Fig. 3.1: Vertical Sieve Shaker

Figure 3.1 shows the laboratory sieve shaker. The sieves are chosen for the size analysis as per requirement, smallest mesh number i.e. coarser sieve is placed at the top and finest sieve i.e. higher mesh number, followed by a pan i.e. final receiver are placed at the bottom. A lid is placed on the top to prevent losses of the sample. The duration of screening can be controlled by an automate timer. During the shaking, the undersize material falls through successive sieves, until it is retained on a sieve having apertures slightly higher than the diameter of the particles. In this way the sample is separated into size fractions.

3.2.2 Ball Mill

The final stage of comminution is preferred in tumbling mills using steel balls as the grinding media and so designated as ball mill (Figure 3.2). Since balls have a more surface area per unit weight than rods, they are appropriate for fine finishing. The term ball mill is restricted to those having a length to diameter ratio 1.5 to 1.0, and less. Mills in which the length to diameter ratio is between 3 to 5 are designated tube mills and instead of balls, rods are used. Several factors influenced the efficiency of ball mill grinding, the pulp density of the feed should be high as possible, during wet grinding. Ball mills should operate between 65 and 80 pct solid by weight, depending on the ore. The rotation speed of the ball mill is 64 rpm.



Fig.3.2: Laboratory Ball Mill

The efficiency of grinding depends on the surface area of the grinding medium used in ball mill. Thus balls should be as small as possible and the charge should be graded such that largest ball just heavy enough to grind the largest and hardest particle in the feed. Grinding balls are usually made of forged or rolled high carbon or alloy steel or cast alloy steel. The grinding medium of ball mill are cast iron balls of 2-5 cm diameter).

3.2.3 X-ray Fluorescence (XRF) Spectrometer

Energy dispersive X-ray fluorescence (XRF) spectrometer is an extremely powerful tool for qualitative and quantitative determination of heavy elements in the presence of each other and in any matrix (Figure 3.3). It is a relatively simple and, in general, non-destructive method for the analytical determination of elements. It is based on the principle that the energy of the emitted X-rays depends on the atomic number (Z) of the element and their intensity

depends on the concentration of the atom in the sample[107]. There are two types of experimental equipment available. One is based on wavelength dispersive XRF and the other is based on energy dispersive XRF. They differ only in the manner the emitted radiation from the sample is dispersed. The wavelength dispersive XRF uses a crystal grating to separate the energies while XRF uses a solid-state detector. XRF has the advantage of speed but the disadvantage of poorer sensitivity and resolution[108].

XRF Spectrometer (Model: EDXRF-800, Make: Shimadzu, Japan, Resolution: 155 eV, Rh target with 5 to 500 kV, 8 samples turret, is available at Metallurgical and Material Engineering Department, M S University of Baroda. Sample analysis range of elements: C to U) is very useful analytical instruments for analysis of both homogeneous and heterogeneous materials, especially for samples of unknown chemistry. XRF unit includes X-ray generator, vacuum unit, automatic collimator, solid state Li detector, sample turret and micro-computer. It is equipped with a high level fundamental parameter (FP) software for qualitative and quantitative analysis of totally unknown sample. The X-ray tube has Rhodium (Rh) target having 5 to 50 kV voltage and 1 to 1000 μ A current range. It makes use of X-rays to excite an unknown sample surface. The EDXRF-800 can automatically identify all elements in a sample based upon a library of X-ray data, i.e., it also contains matching software providing standard less analysis. The energy level indicates the element involved, and the number of pulses counted at each energy level over the entire counting time is related to the concentration of the element. Sample can be analysed either in air or vacuum or helium. For quantitative analysis, either of the two techniques namely fundamental parameter (FP) method or calibration curve (CC) method can be used. The later method is more accurate than the former one. XRF technique is inherently very precise and is attractive for elements which lack reliable wet chemical methods, such as tantalum and rare earths.



Fig. 3.3: XRF- 800

3.2.4 Scanning Electron Microscopy (SEM)

Scanning electron microscopy (SEM) is used primarily for the study of surface topography of solid materials. It permits a depth of field far greater than optical or transmission electron microscopy (TEM). The resolution of the SEM is about 3 nm, approximately two orders of magnitude greater than the optical microscope and one order of magnitude less than the TEM. Thus, the SEM bridges the gap between the other two techniques[108].

Scanning electron microscopic examinations of the powder samples of various wastes as received were carried out to observe the size and shape morphology using JEOL SEM (Model: JSM-5610 LV) coupled with Oxford Energy Dispersive Analytical X-ray (EDAX) system, which is available at Metallurgical and Materials Engineering Department, M. S. University of Baroda, Vadodara. Further, reduced pellets were also observed under SEM. Few photographs of SEM observations were taken.

3.2.5 X-ray Diffractometer

The diffraction of X-ray is of great analytical significance, as it is used to obtain information about the structure, composition, and state of poly-crystalline materials. XRD (X-ray Diffractometer) is adaptable to quantitative applications, because the intensities of the diffraction peaks of a given compound in a mixture are proportional to the fraction of the material in the mixture[107]. X-ray diffractometers are basically analogous to an optical grating spectrometer, with the difference that lenses and mirrors are not used with X-rays. Therefore,

they appear quite different from their counterparts. X-Ray Diffractometer Advance -8, D8 Advance Bruker (Make).

The LYNXEYE XE-T is based on silicon strip technology and features an unmatched energy resolution to identify the phases present in samples, this type XRD is available at Sophisticated Instrumentation Centre for Applied Research and Testing (SICART), Vallabh Vidyanagar.

3.2.6 Air Classifier

Laboratory Air Classifier:

Air Inlet Size: 100 mm diameter

Air Outlet Size: 249 mm diameter, outside

The mechanism of separation of gangue minerals from the valuable mineral, occurring within the cyclone is known as classification. Cyclones utilise centrifugal force to increase the settling rate of particles. Although the objective of cyclone operation is to separate particles by size, particle density, particle shape and other factors also affect the settling rate of particles and hence cyclone performance. Cyclones are used in preference to screens as a means of size separation in the grinding circuit as they are more efficient at fine separation sizes. Figure 3.4 shows air classifier.



Fig.3.4: Laboratory Air Classifier

3.2.7 Hydro-Classifer (Centrifugal Classifier)

This is continuously operating classifying device that utilises centrifugal force to accelerate the settling rate of particles. It is one of the important devices in the minerals industry, its main use in mineral processing being as a classifier, which has proved extremely efficient at fine separation sizes.

A typical hydro-cyclone (fig) consists of a conically shaped vessel, open at its apex, or underflow, joined to a cylindrical section, which has a tangential feed inlet. The top of the cylindrical section is closed with a plate through which passes an axially mounted overflow pipe. The pipe is extended into the body of cyclone by a short, removable section known as the 'Vortex Finder', which prevents short-circuiting of feed directly into the overflow. Schematic of hydraulic classifier is shown in Figure 3.5.

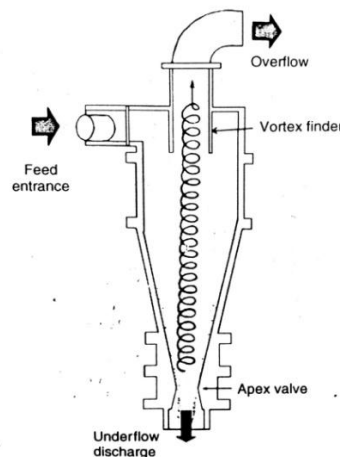


Fig. 3.5: Schematic of Hydraulic Classifier

The feed is introduced under pressure through the tangential entry which imparts a swirling motion to the pulp. This generates a vortex in the cyclone, with a low-pressure zone along the vertical axis. An air core develops along the axis, generally connected to the atmosphere through the apex opening, but in part created by dissolved air coming out of solution in the zone of low pressure. The centrifugal force developed accelerates the settling rate of the particles, thereby separating particles according to size and specific gravity. Particles with faster settling rate move to the wall of cyclone, where the velocity is lowest, and drift to the apex opening. Due to the action of drag force, particles with slower settling rate move towards the zone of low pressure along the axis and are carried upward through the vortex finder to the overflow.



Fig. 3.6: Laboratory Hydro-cyclone

3.2.8 Wilfley Tabling

Laboratory model table (1016X457mm Denver Wilfley Table) is shown in Figure 3.7. The Tabling works on the principle of gravity separation technique. It is also known as *Shaking Table*. When a flowing film of water flows over a flat, inclined surface the water close to the surface is retarded by the friction of water flows on the surface; the velocity increases towards the water surface. If mineral particles are introduced into the film, small particles will not move as rapidly as large particles, since they will be submerged in the slower moving portion of the film. Particles of high specific gravity will move more slowly than lighter particles, and so a lateral displacement of material will be produced. The flowing film effectively separates coarse light particles from small dense particles, and the mechanism is utilized to some extent in the shaking table concentrator, which is perhaps the most metallurgically efficient form of gravity concentrator.



Fig. 3.7: Laboratory Wilfley Table

It consists of slightly inclined deck, on to which feed, at about 25pct solids by weight, is introduced at the feed box and is distributed along; wash water is distributed along the balance of the feed side from launder. The table is vibrated longitudinally, by the mechanism, using a slow forward stroke and a rapid return, which causes the mineral particles to CRAWL along the deck parallel to the direction of motion. The minerals are thus subjected to two forces that due to the table motion and that, at right angles to it, due to the following film of water(Figure 3.8).The net effect is that the particles move diagonally across the check from the end and, since the effect of the flowing film depends on the size and density of the particles, they will fan out on the table, the smaller, denser particles riding highest towards the concentrate launder at the far end, while the larger lighter particles as washed into the tailing launder, which runs along the length of the table.

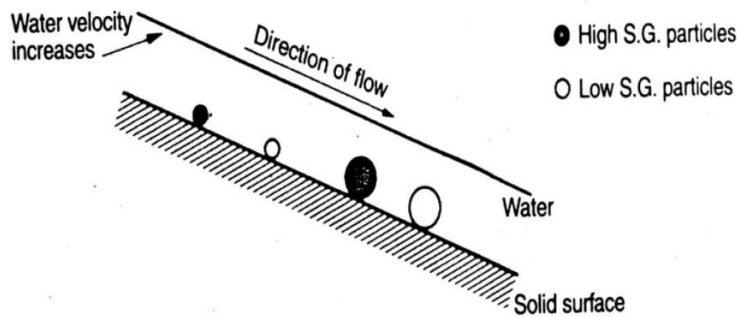


Fig. 3.8: Actions in Flowing Particles

Laboratory Wilfley Table:

Stroke Length: 8 cm

Speed of Table: 101 stroke/min

Flow Rate: $14-22 \times 10^{-5} \text{ m}^3/\text{s}$

Angle of Table: 30°

3.3 Characterization

3.3.1 Size Analysis

Sludge (obtained from Steel Plant) was associated with moisture and non-uniform particles sizes. Since raw materials (i.e. dust and sludge, coal) have non-uniform particles sizes. After drying and grinding at the ball mill, the samples were taken to a suitable size. Size analyses of raw materials were carried out in sieve shaker for 15 minutes. In each case, 100 g sample was taken. Results of size analyses for JSW Dust, JSW Sludge VIZAG Sludge and coal are presented in Tables 3.3,3.4, 3.5 and 3.6 respectively.

Table 3.3: Size analysis of JSW Dust

ASTM Mesh No.	Particle Size, μm	Weight pctretained	Cumulative pct retained	Cumulative pct passing
85	180	81.7	81.7	18.3
100	150	6.5	88.2	11.8
150	106	7.0	95.2	4.8
200	75	2.3	97.5	2.5
Pan		2.5	100.0	

Table 3.4: Size analysis of JSW Sludge

ASTM Mesh No.	Particle Size, μm	Weight pctretained	Cumulative pct retained	Cumulative pct passing
85	180	65.4	65.4	34.6
100	150	11.1	76.5	23.5
150	106	13.4	89.9	10.1
200	75	5.1	95.0	5.0
Pan		5.0	100.0	

Table 3.5: Size analysis of VIZAG Sludge

ASTM Mesh No.	Particle Size, μm	Weight pct retained	Cumulative pct retained	Cumulative pct passing
85	180	54.8	54.8	45.2
100	150	11.6	66.4	33.6
150	106	17.5	83.9	16.1
200	75	8.2	92.1	7.9
Pan		7.9	100.0	

Table 3.6: Size analysis of Coal

ASTM Mesh No.	Particle Size, μm	Weight pct retained	Cumulative pct retained	Cumulative pct passing
85	180	89.8	89.8	10.2
100	150	6.6	96.4	3.6
150	106	1.5	97.9	2.1
200	75	1.2	99.1	0.9

Pan		0.9	100.0	
-----	--	-----	-------	--

3.3.2 Chemical Analysis

The objective of chemical analysis was to determine the chemical composition of the raw materials by different established techniques. Studies were carried out either on the samples as received or after drying. Each material(individually) was thoroughly mixed after drying and a representative sample was collected from mixed material for detailed investigation.

Chemical analysis of Steel Plant's dust and sludge were carried out by Energy Dispersive X-ray Fluorescence (XRF) Spectrometer (Model:EDXRF-800, Make: Shimadzu, Japan); which is available at Metallurgical and Materials Engineering Department, M. S. University of Baroda, Vadodara.

Measurement conditions were as follows:

1. Sample: Powder form,
2. Atmosphere: Vacuum,
3. Temperature: Liquid nitrogen,
4. Collimator: 10 mm.

X-ray fluorescent spectrometer (XRF) is used to determine the Chemical compositions of the samples. The chemical analyses of the Steel Plant's waste samples are shown in Table 3.7. Proximate analysis of coal is carried out in laboratory as per standard method (ASTM D3172) and presented in Table 3.8.

Table 3.7: Chemical analysis of waste samples (as received)

Assay	Fe(T) pct	Fe ₂ O ₃ pct	CaO pct	SiO ₂ pct
Dust from Jindal Steel Works, Bellari	38.77	55.39	35.84	5.57
Sludge from Jindal Steel Works, Bellari	51.64	73.77	20.69	2.51
Sludge from Vizag Steel plant, Vishakhapatnam	49.49	70.70	23.29	1.65

Table 3.8: Proximate analysis of coal samples (as received)

Analyte	Moisture	Volatile Matter	Ash	Fixed carbon
Wt. %	1.0	17.0	20.0	62.0

3.3.3 Microscopic Observation of Raw Materials

Scanning electron microscopy (SEM) is used primarily for the study of surface topography of solid materials. It permits a depth of field far greater than optical or transmission electron microscopy (TEM).

Operational condition of the JEOL SEM:

Model: JSM-5610 LV

High Vacuum mode (HV)

Resolution (SEI) 5.0 nm

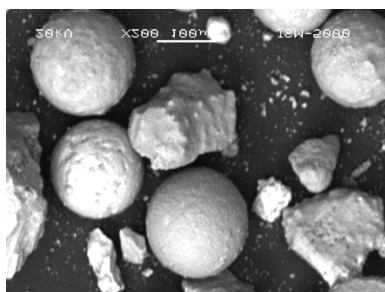
Accelerating Voltage: 30 kV

Working Distance: 6 mm

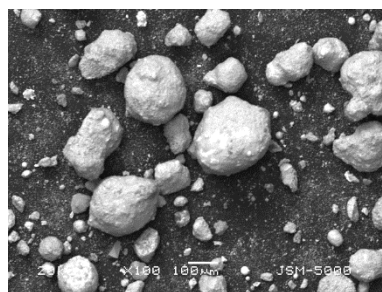
Magnification: 25x to 300,000x

Scanning electron microscopic examinations of the powder samples of JSW dust and JSW sludge and VIZAG sludge were carried out to observe the size and shape morphology using JEOL SEM.

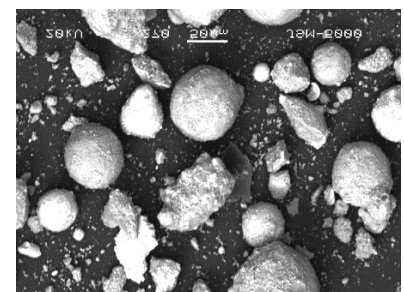
Microscopic observation of dust and sludge materials were done by Scanning Electron Microscope (SEM) at Metallurgical and Materials Engineering Department, M. S. University of Baroda, Vadodara. The Scanning Electron Microscopic (SEM) photo-micrographs of JSW Dust, JSW Sludge and VIZAG Sludge are shown in Figure 3.9(a-c). Figure 3.9(a) shows the SEM photomicrographs of JSW Dust sample depicting the presence of mostly spheroidal shaped particles, some particles are also irregular in shape. JSW sludge and Vizag sludge samples are shown in Figures 3.9(b and c) respectively, that shows spheroidal and irregular shaped particles. The particles are separate from each other.



(a) JSW Dust



(b) JSW Sludge



(c) VIZAG Sludge

Fig: 3.9: SEM micrographs of JSW Dust, JSW Sludge and VIZAG Sludge samples

3.3.4 XRD Analysis

A few samples were selected for X-ray diffraction studies. Samples were collected and by hand grinding, they were powdered and spread on a glass slide coated with thin film of silicon grease. With the help of another slide, the powder was spread uniformly on the slide. Then the sample was placed in the holding chamber for X-ray diffraction. The Cu K α monochromatic X-ray radiations were utilized to record the XRD spectrum of samples over spectral span of 10 to 80°. X-rays were generated by imposing 1.0 kV potential difference across the cathode, while maintaining a generator current at 300 mA. The wavelength of X-rays generated with Cu target was 1.5406 Å. The step size and scan speed were 0.010 and 3 degree/min respectively. Diffraction pattern was recorded, and the phase identification was carried out by matching the peaks with powder diffraction patterns given in Powder Diffraction Handbooks (sets 1-30), published by Joint Committee on Powder diffraction Standards, Philadelphia, Pennsylvania, USA.

XRD analysis of dust and sludge were carried out to identify the phase distribution in the raw material. The results of XRD analysis for JSW dust and JSW sludge are shown in Figures 3.10 and 3.11. Further the peaks are indexed as per JCPDS data book and tabulated in Tables 3.9 and 3.10 respectively.

(Coupled TwoTheta/Theta)

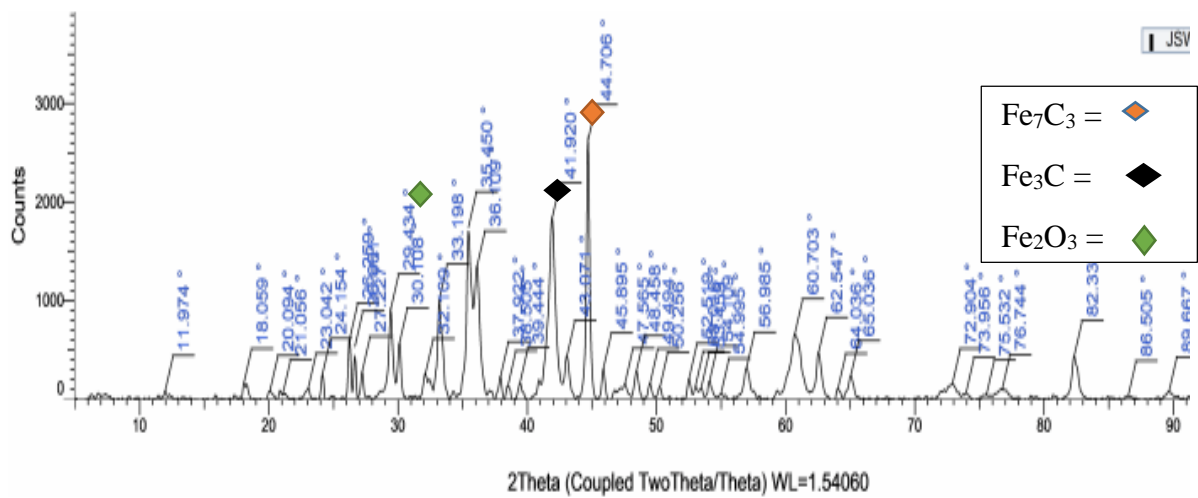


Fig. 3.10: XRD Analysis of JSW Dust (Original Sample)

Table 3.9: XRD analysis of JSW Dust

Sr.No.	d Value Observed	Relative Intensity Observed	d Value (Theoretical)	Relative Intensity (Theoretical)	Phases Present
1	2.28	6.1	2.27	8	Fe ₇ C ₃
2.	2.02	100	2.02	100	Fe ₇ C ₃
3.	1.17	16.5	1.171	16	Fe ₇ C ₃
4	2.15	69.8	2.16	60	Fe ₃ C
5	2.53	66.3	2.52	70	Fe ₂ O ₃
6	1.483	17.8	1.489	22	Fe ₂ O ₃

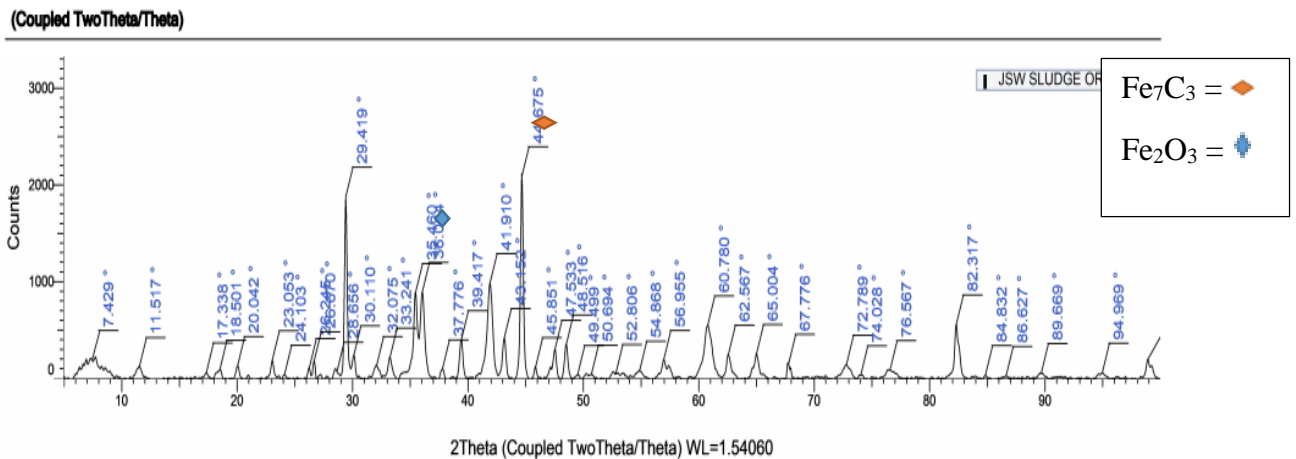


Fig. 3.11: XRD Analysis of JSW Sludge (Original Sample)

Table 3.10: XRD analysis of JSW Sludge

Sr.No.	d Value Observed	Relative Intensity Observed	d Value (Theoretical)	Relative Intensity (Theoretical)	Phases Present
1	2.02	100	2.02	100	Fe ₇ C ₃
2.	1.38	7.1	1.35	8	Fe ₇ C ₃
3.	1.17	26.6	1.17	16	Fe ₇ C ₃
4.	2.28	18.8	2.208	17	Fe ₂ O ₃
5	2.15	47.1	2.12	40	Fe ₂ O ₃
6	1.61	9.1	1.60	8	Fe ₂ O ₃
7	2.09	19.9	2.09	20	Fe ₃ O ₄

The peaks are not sharp in all the XRD plot for samples, which confirms the samples are amorphous in nature. As amorphous materials do not possess periodicity and atoms are randomly distributed in 3D space. So in amorphous phase X-ray will be scattered in many directions leading to a large bump distributed in a wide (2 theta) range instead of high intensity narrower peaks[109].

After detailed characterization following features were observed(in general) regarding dust and sludge.

- The size of the dust and sludge was not uniform.
- Along with Fe bearing particles, lime and silica were the major constituents.

- SEM of the original samples reveals that the particles in dust and sludge are of globular shapes and are not associated with any other phase.
- XRD results of the same confirms that the samples are amorphous and not crystalline.

3.4 Beneficiation

The size distribution of all the wastes were non-uniform; from 66.4 pct in VIZAG sludge to 88.2 pct in JSW dust were found above 150 μm (i.e. 100 mesh). To get uniformity in particle size the dust and sludge was grinded in ball mill up to 150 μm (i.e. 100 mesh). Sufficient number of balls of different sizes, small and large (cast iron balls of 2-5 cm diameter), were put into the ball mill with rotation 64 rpm.. The milling time was 14 to 15 hours. The impact of balls on the material produced the dust and sludge powder. Size analysis of wastes and coal after grinding are shown in Tables 3.11 to 3.14.

Table 3.11: Size analysis of JSW Dust (After grinding)

ASTM Mesh No.	Particle Size, μm	Weight pct retained	Cumulative pct retained	Cumulative pct passing
100	150	1.8	1.8	98.2
Pan		98.2	100.0	

Table 3.12: Size analysis of JSW Sludge (After grinding)

ASTM Mesh No.	Particle Size, μm	Weight pct retained	Cumulative pct retained	Cumulative pct passing
100	150	1.4	1.4	98.6
Pan		98.6	100.0	

Table 3.13: Size analysis of VIZAG Sludge (After grinding)

ASTM Mesh No.	Particle Size, μm	Weight pct retained	Cumulative pct retained	Cumulative pct passing
100	150	1.7	1.7	98.3
Pan		98.3	100.0	

Table 3.14: Size analysis of Coal (After grinding)

ASTM Mesh No.	Particle Size, μm	Weight pct retained	Cumulative pct retained	Cumulative pct passing
100	150	0.6	0.6	99.4
Pan		99.4	100.0	

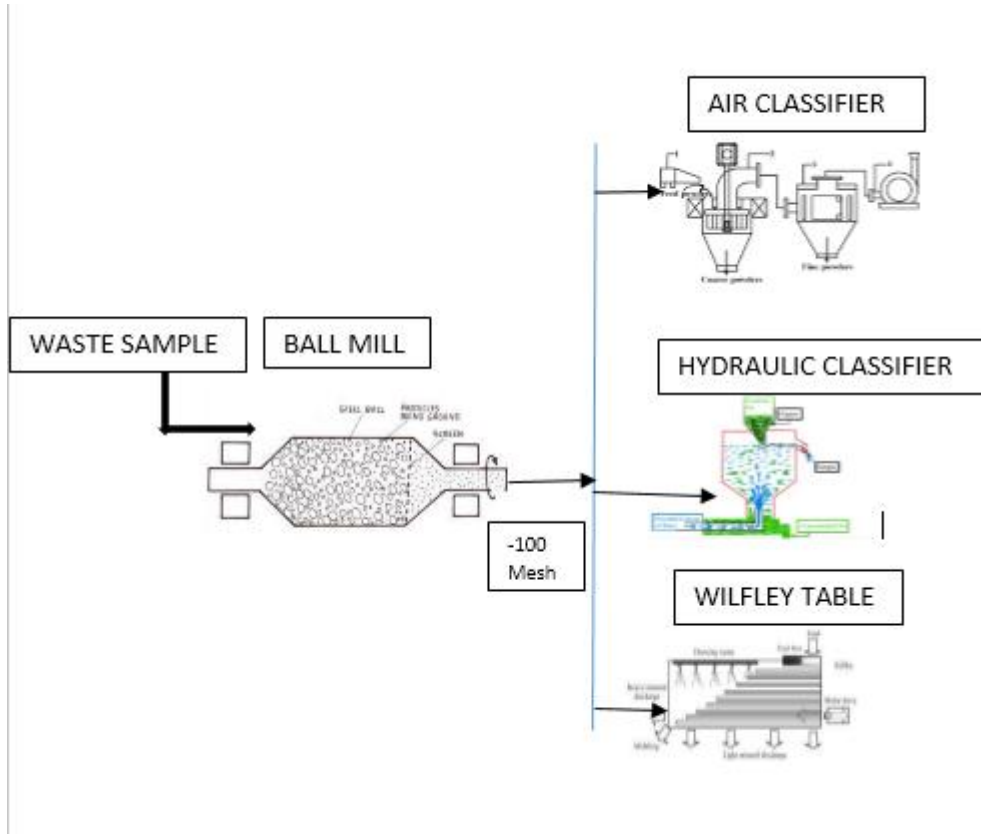


Fig. 3.11A: Flow diagram of single stage beneficiation

3.4.1 Single Stage Beneficiation Method

To upgrade the iron (Fe) value in steel plant wastes, many trials are taken for beneficiation processes to discard gangue materials. The beneficiation methods of powder samples were carried out by hydraulic classifier, air classifier and Wilfley table (**Figure 3.11A**). All the experiments are carried out at Metallurgical and Materials Engineering Department, MSU Vadodara as per the standard procedures. Recovery of iron from wastes were calculated as follows:

$$\text{Iron recovery (pct)} = \left\{ \frac{(W_2 \times f_2) \times 100}{(W_1 \times f_1)} \right\} \quad \dots(3.1)$$

Where W_1 is weight of feed sample, W_2 is weight of product after beneficiation,

f_1 is fraction of $\text{Fe}_{(T)}$ in feed sample, and f_2 is fraction of $\text{Fe}_{(T)}$ in product after beneficiation.

The sample is tested for Centrifugal classifier, air classifier and wilfley table. The air classifier is having air Inlet Size : 100mm diameter Air Outlet Size : 249 mm diameter, outside. Wilfley table is made in lab of stroke length : 8cm, Speed of Table 101 stroke/min, Flow Rate : $14-22 \times 10^{-5} \text{ m}^3/\text{s}$ and table angle : 30°

Results for each beneficiation method used for all three samples are shown in Tables 3.15 to 3.19.

Table 3.15: Result of Centrifugal Classifier [Initial weight: 500g(W₁)]

Assay →	Initial Fe _{(T),pct} (f ₁)	Final Fe _{(T),pct} (f ₂)	Final Fe ₂ O ₃ , pct	CaO,pct	SiO ₂ ,pct	Weight under flow, g(W ₂)	Recovery, pct
JSW Dust	38.77	45.77	65.39	25.63	2.80	392.0	92.56
JSW Sludge	51.64	53.15	75.93	18.88	2.46	441.6	90.90
Vizag Sludge	49.49	50.97	72.81	26.70	2.12	355.0	73.12

Table 3.16: Result of Air Classifier [Initial weight: 200g (W₁)]

Assay →	Initial Fe _{(T),pct} (f ₁)	Final Fe _{(T),pct} (f ₂)	Final Fe ₂ O ₃ , pct	CaO,pct	SiO ₂ ,pct	Weight under flow, g(W ₂)	Recovery, pct
JSW Dust	38.77	46.24	66.05	7.70	3.96	159.26	94.97
JSW Sludge	51.64	52.03	74.33	18.43	2.76	162.25	81.74
Vizag Sludge	49.49	47.95	68.5	8.49	2.19	170.08	82.39

Table 3.17: Result of Tabling for JSW Dust[Initial weight: 200g (W_1) and Initial $Fe_{(T),pct}$ (f_1): 38.77]

Assay	Final $Fe_{(T),pct}(f_2)$	Final Fe_2O_3, pct	CaO,pct	SiO ₂ ,pct	Final weight, g (W_2)	Recovery, pct
Concentrate	45.57	65.10	18.56	5.12	73.10	42.96
Middling	30.64	43.77	24.23	3.26	68.60	27.11
Tailings	28.67	40.96	32.36	4.64	45.00	16.64

Table 3.18: Result of Tabling for JSW Sludge[Initial weight(W_1): 200g and Initial $Fe_{(T),pct}$ (f_1): 51.64]

Assay	Final $Fe_{(T),pct}(f_2)$	Final Fe_2O_3,pct	CaO,pct	SiO ₂ ,pct	Final weight, g (W_2)	Recovery,pct
Concentrate	60.45	86.36	12.03	0.50	97.10	56.83
Middling	49.40	70.57	5.30	2.03	27.72	13.26
Tailings	48.90	69.86	22.60	3.0	51.80	24.53

Table 3.19: Result of Tabling for Vizag Sludge[Initial weight(W_1): 200g and Initial $Fe_{(T),pct}$ (f_1): 49.49]

Assay	Final $Fe_{(T),pct}(f_2)$	Final Fe_2O_3, pct	CaO,pct	SiO ₂ ,pct	Final weight, g (W_2)	Recovery, pct
Concentrate	60.08	85.83	11.18	2.84	84.35	51.20
Middling	54.90	78.43	20.02	1.23	48.98	27.17
Tailings	34.89	49.84	32.66	4.37	42.72	15.06

Further all the beneficiation methods for each sample were compared and shown in Table 3.20 to 3.22. It was found that for JSW Dust air classifier was most suitable, total Fe increased from 38.77 to 46.24pct. Tabling gave good result for JSW sludge, total Fe increased from 51.64 to 60.45 pct. Again, for VIZAG Sludge Tabling was most suitable, total Fe increased from 49.49

to 60.08pct. However, Air Classifier was very much useful beneficiation process to reduce gangue materials in general and in particular CaO

Table 3.20: Results of JSW Dust with various beneficiation processes

Process	Final Fe _(T) ,pct(f ₂)	Final Fe ₂ O ₃ , pct	CaO,pct	SiO ₂ ,pct	Recovery,pct
Original Sample	38.77	55.39	35.84	5.57	
Centrifugal Classifier	45.77	65.39	25.63	2.80	92.56
Air Classifier	46.24	66.05	7.70	3.96	94.97
Tabling Concentrate	45.57	65.10	18.56	5.12	42.96

Table 3.21: Results of JSW Sludge with various beneficiation processes

Process	Final Fe _(T) ,pct(f ₂)	Final Fe ₂ O ₃ , pct	CaO,pct	SiO ₂ ,pct	Recovery,pct
Original Sample	51.64	73.77	20.69	2.51	
Centrifugal Classifier	53.15	75.93	18.88	2.46	90.90
Air Classifier	52.03	74.33	18.43	2.76	81.74
Tabling Concentrate	60.45	86.36	12.03	0.50	56.83

Table 3.22: Results of VIZAG Sludge with various beneficiate on processes

Process	Final Fe _(T) , pct (f ₂)	Final Fe ₂ O ₃ , pct	CaO, pct	SiO ₂ , pct	Recovery, pct
Original Sample	49.49	70.70	23.29	1.65	
Centrifugal Classifier	50.97	72.81	20.20	2.12	73.12
Air Classifier	47.95	68.50	8.49	2.19	82.39
Tabling Concentrate	60.08	85.83	11.18	2.84	51.20

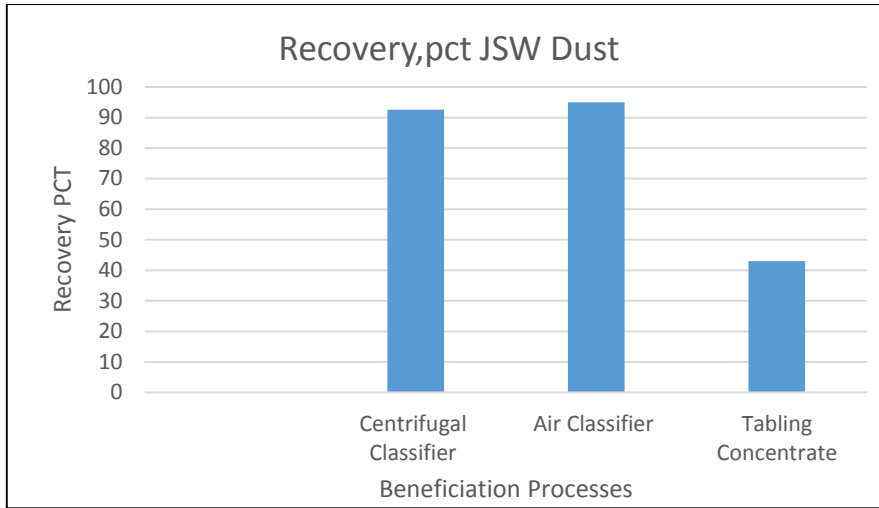


Fig. 3.12: Results of various beneficiation processes for JSW Dust

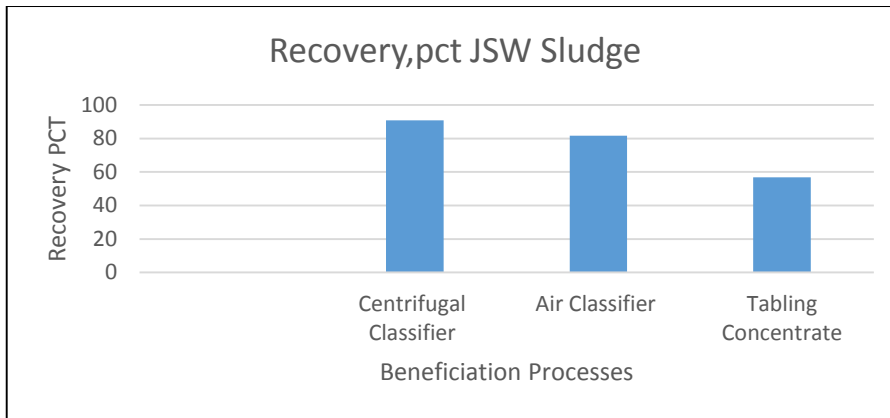


Fig. 3.13: Results of various beneficiation processes for JSW Sludge

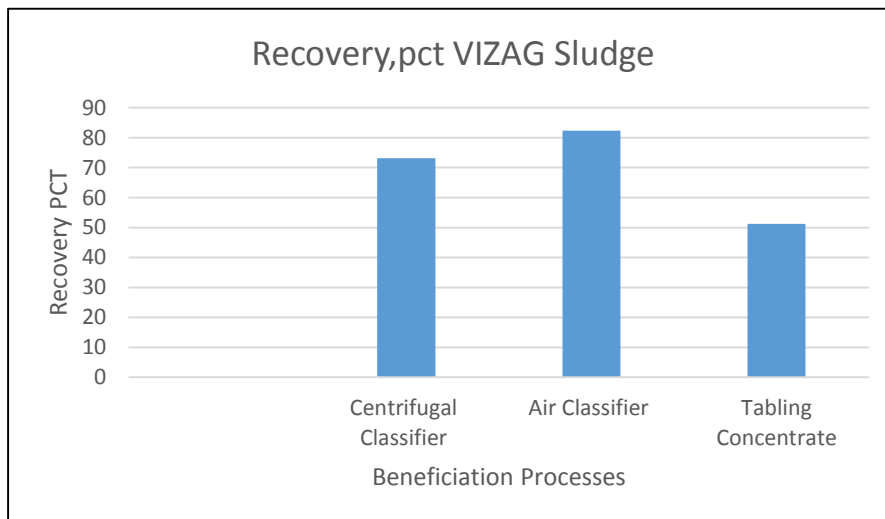


Fig. 3.14: Results of various beneficiation processes for VIZAG Sludge

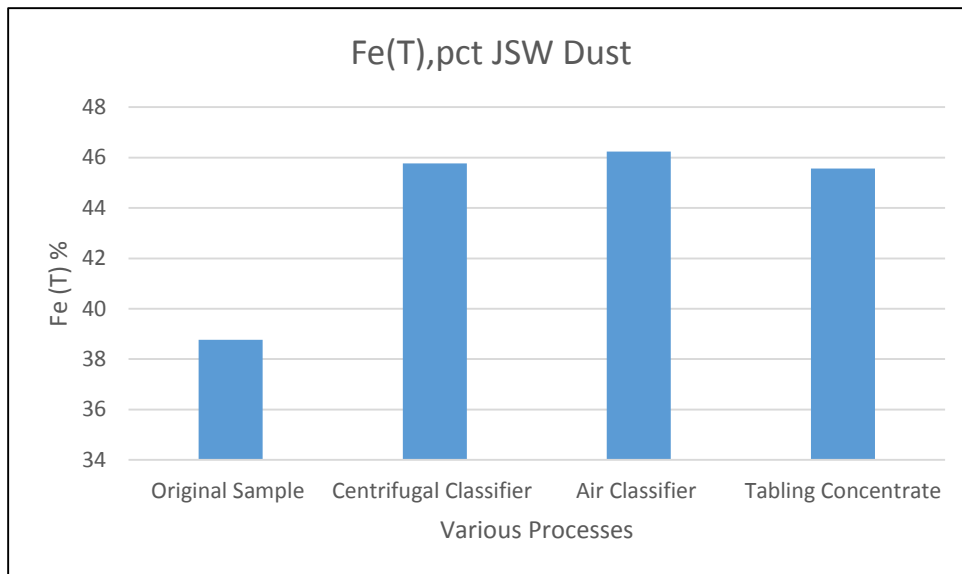


Fig. 3.15: Fe(T)% after various beneficiation processes for JSW Dust

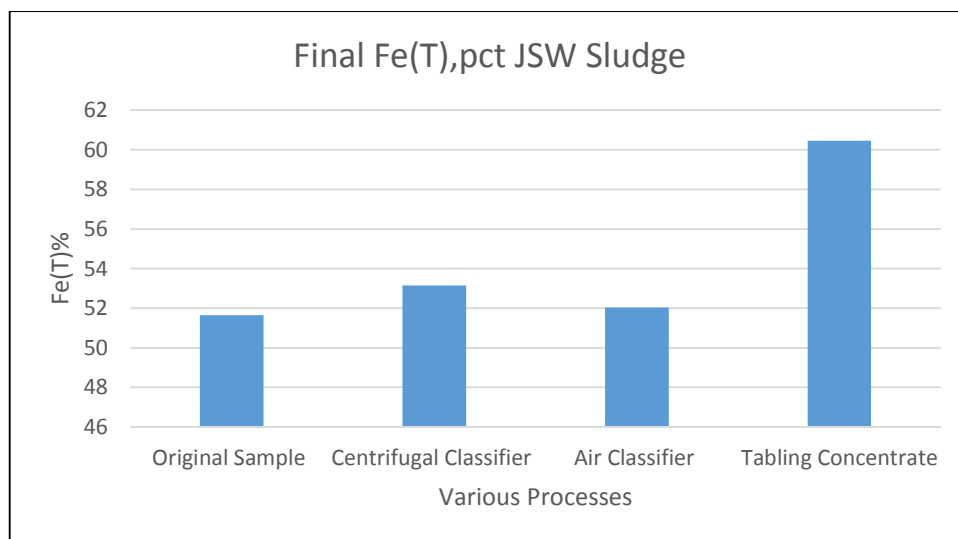


Fig. 3.16: Fe(T)% after various beneficiation processes for JSW Sludge

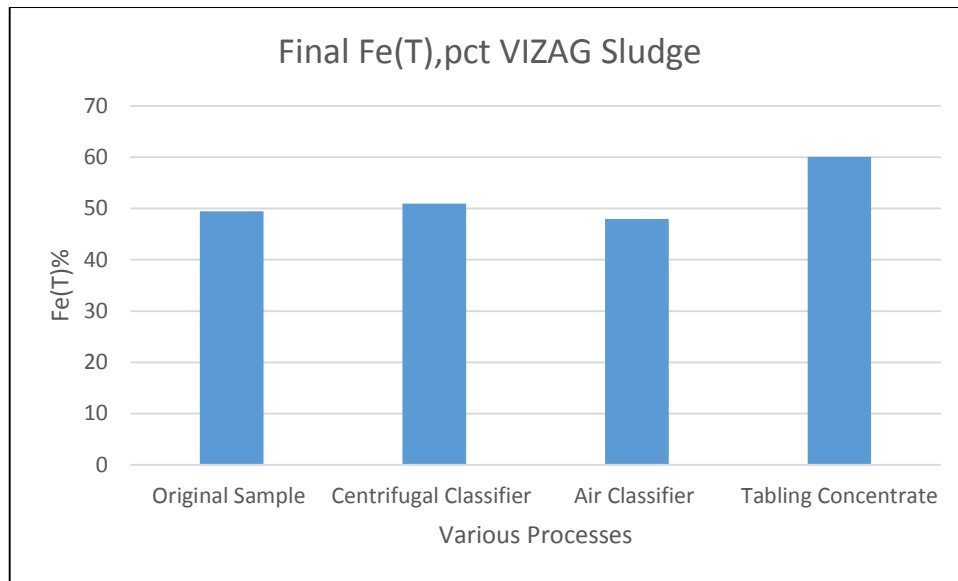


Fig. 3.17: Fe(T)% after various beneficiation processes for VIZAG Sludge

The result shown in Figure 3.12 to 3.17 explains that air classifier is giving the best result in terms of recovery and Fe(T)% for all the wastes and that may be because the waste is having lime and silica as major constituent other than Fe bearing particles. Due to grinding of the dust and sludge particles were below 150 μm sizes and then subjected to air classifier the lightweight particles of lime ($\rho_{\text{CaO}} = 3.34 \text{ g.cm}^{-3}$) and silica ($\rho_{\text{SiO}_2} = 2.65 \text{ g.cm}^{-3}$) would have easily separate out as the overflow; heavy-weight particles of iron oxide ($\rho_{\text{Fe}_2\text{O}_3} = 5.24 \text{ g.cm}^{-3}$) were separate out as underflow. Considering the results of individual process on all the three types of waste, a common two stage beneficiation route was developed.

3.4.2 Two Stage Beneficiation Method

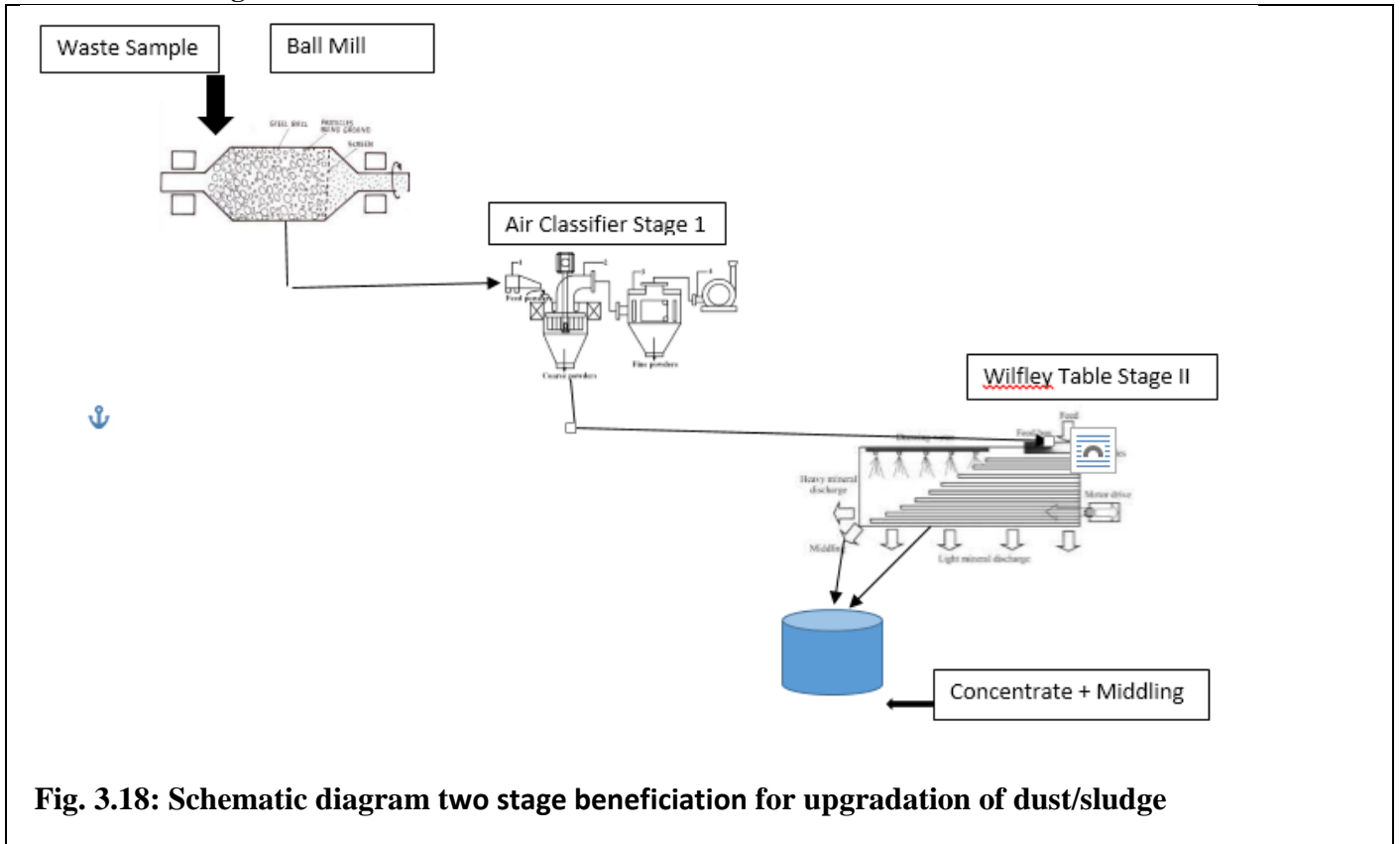


Fig. 3.18: Schematic diagram two stage beneficiation for upgradation of dust/sludge

The results of two stage beneficiation are given in Table 3.23 to 3.25 for JSW dust, JSW sludge and VIZAG sludge respectively. Maximum increased in total Fe was 63.48 pct (for Tabling concentrate) achieved in JSW sludge; for JSW dust Fe total was upgraded to 61.13 pct (for concentrate + middling of Tabling); and in VIZAG sludge was upgraded to 60.04 pct (for Tabling concentrate) total Fe. Based on total Fe percentage, the two stage beneficiation route is selected.

- Stage 2 recovery is calculated with result of stage 1 as the initial value
- Fe (pct)for (Concentrate + Middling) = $\left\{ \frac{(W_c \times Fe_c + W_m \times Fe_m) \times 100}{(W_c + W_m)} \right\} \dots (3.2)$

where W_c is weight of concentrate, W_m is weight of middling;

Fe_c is fraction of $Fe_{(T)}$ in concentrate, and Fe_m is fraction of $Fe_{(T)}$ in middling.

Table 3.26 shows the final Fe_2O_3 , pct considered for pellet production.

Table 3.23: Result of two stage beneficiations for JSW DUST

Process		Initial weight, g	Fe _(T) ,pct	Fe ₂ O ₃ ,pct	Weight retained, g	Recovery, pct
	Original Sample		38.77	55.39		
Stage 1	Air Classifier underflow	200	46.24	66.05	159.26	94.97
Stage 2	Tabling Concentrate	149.26	62.16	88.80	54.55	49.15
Stage 2	Tabling Middling		60.04	85.77	51.35	44.67
Final output	Concentrate + Middling		61.13	87.33	105.9	93.8

Table 3.24: Result of two stage beneficiations JSW SLUDGE

Process		Initial weight, g	Fe _(T) , pct	Fe ₂ O ₃ , pct	Weight retained, g	Recovery, pct
	Original Sample		51.64	73.77		
Stage 1	Air Classifier	200	53.25	76.07	162.25	83.65
Stage 2	Tabling Concentrate	152.25	63.48	90.69	100.12	78.39
Stage 2	Tabling Middling		59.75	85.36	18.57	13.66
Final output	Concentrate + Middling		62.89	89.84	118.69	92.07

Table 3.25: Result of two stage beneficiation VIZAG SLUDGE

Process		Initial weight, g	Fe _(T) ,pct	Fe ₂ O ₃ ,pct	Weight retained, g	Recovery, pct
	Original Sample		49.49	70.70		
Stage 1	Air Classifier	200	47.95	68.5	170.08	82.39
Stage 2	Tabling Concentrate	160.0	60.04	85.77	73.75	57.72
Stage 2	Tabling Middling		37.36	53.37	37.78	18.4
Final output	Concentrate + Middling		52.36	74.80	111.53	76.12

Table 3.26: Final Fe₂O₃, pct considered for pellet production

Assay →	Initial Fe _(T) ,pct(f ₁)	Final Fe _(T) ,pct (f ₂)	Final Fe ₂ O ₃ ,pct
JSW Dust	38.77	61.13	87.33
JSW Sludge	51.64	63.48	90.69
Vizag Sludge	49.49	60.04	85.77

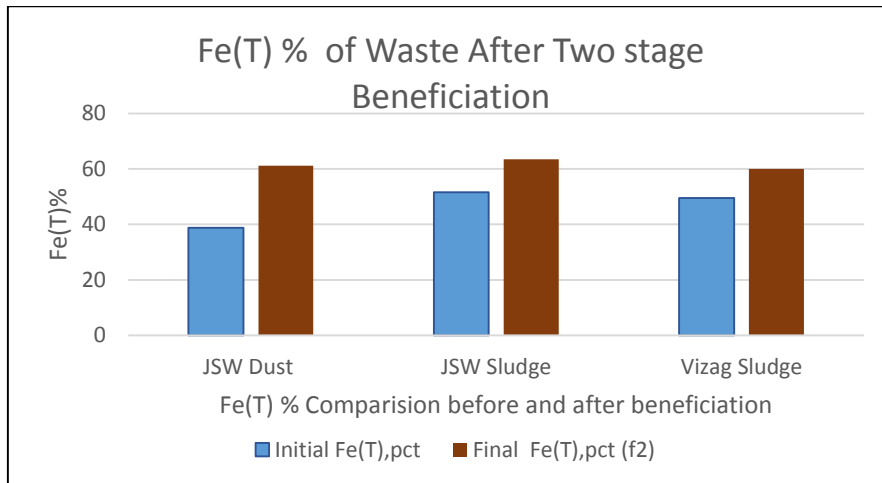


Fig. 3.19: Fe(T)% after two stage beneficiation for all the waste

After finalizing the two stage beneficiation route, all the three types of waste were processed accordingly. After the processing it was observed that in case of JSW dust, JSW Sludge and

VIZAG Sludge there was increase in percentage of Fe_2O_3 up to 87.33 pct, 90.69 pct and 85.77 pct from initial Fe_2O_3 55.39 pct, 73.77 pct and 70.70 pct respectively.

3.5 Conclusions

1. The steel plant wastes (like JSW dust, JSW sludge and VIZAG sludge) can be easily beneficiated for the upgradation of the iron (Fe) values.
2. For single stage beneficiation method: i) JSW dust improved the iron (Fe) values from 38.77 pct to 46.24 pct by Air Classifier with 94.97 pct recovery; ii) JSW sludge improved the iron (Fe) values from 51.64 pct to 60.45 pct by Tabling with 56.83 pct recovery ; and iii) VIZAG sludge improved the iron (Fe) values from 49.49 pct to 60.08 pct by Tabling with 51.2 pct recovery.
3. For two stage beneficiation method (i.e, air classifier was used in the first stage and the underflow of air classifier was treated again in Wilfley Table): i) JSW dust improved the iron (Fe) values up to 61.13 pct (concentrate + middling) with 93.8 pct recovery; ii) JSW sludge improved the iron (Fe) values up to 63.48 pct (concentrate) with 78.39 pct recovery ; and iii) VIZAG sludge improved the iron (Fe) values up to 60.04 pct (concentrate) with 57.72 pct recovery.
4. After two stage beneficiation method, it was observed that in case of JSW dust, JSW Sludge and VIZAG Sludge there was increase in percentage of Fe_2O_3 up to 87.33 pct, 90.69 pct and 85.77 pct from initial Fe_2O_3 55.39 pct, 73.77 pct and 70.7 pct respectively.
5. These upgraded steel plant wastes are taken for further studies.